SUPPLEMENTARY INFORMATION

Directing the size and dispersity of silver nanoparticles with kudzu leaf extracts

Jaley Faith Adkins[a], Amandeep Kaur[a], Md. Sofiul Alom[a], Haridas Chandran[b], Farshid Ramezanipour[a], and Andrew J. Wilson[a*]

[a.] Department of Chemistry, University of Louisville, Louisville, Kentucky, 40292, United States

[b.] Belfry High School, Belfry, Kentucky, 41514, United States

*Corresponding author e-mail: aj.wilson@louisville.edu

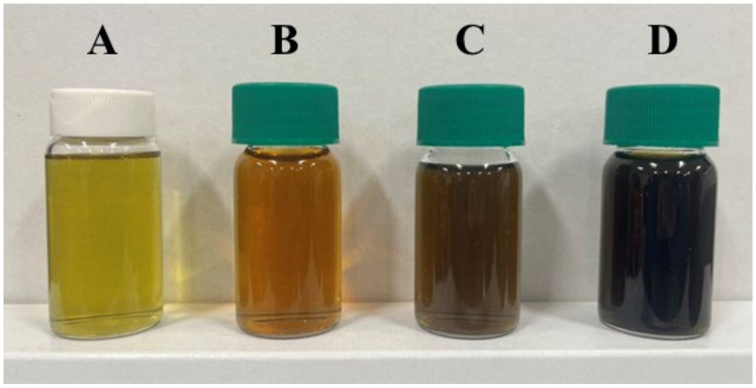

Figure S1. Colloids of Ag nanoparticles synthesized with final concentrations of 0.33 mM $AgNO_3$ and 16.5 %v/v of (A) ethanolic kudzu leaf extract, (B) aqueous kudzu leaf extract, (C) ethanolic chlorophyllin standard, and (D) aqueous chlorophyllin standard.

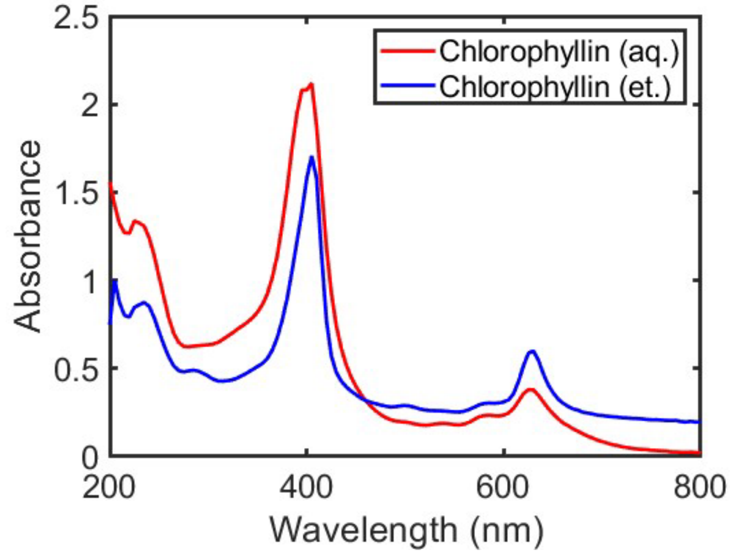

Figure S2. UV-visible spectra of aqueous (red curve) and ethanolic (blue curve) chlorophyllin standards.

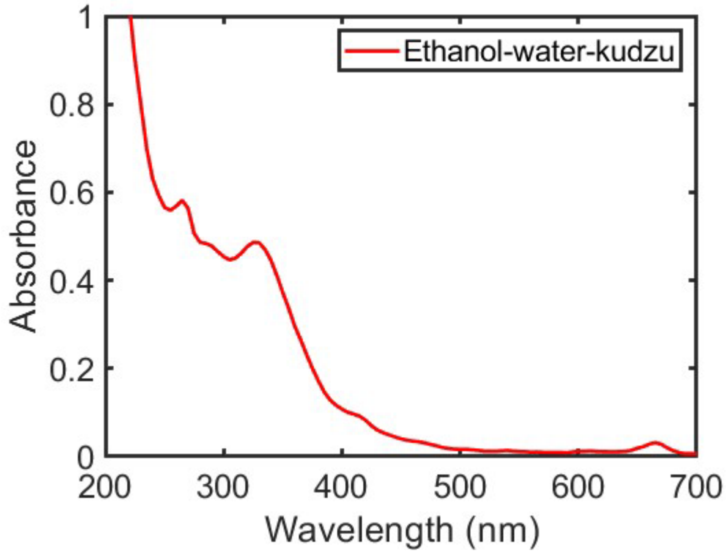

Figure S3. Absorbance spectra of a kudzu leaf extract prepared using a solvent composed of equal volumes of H_2O and CH_3CH_2OH.

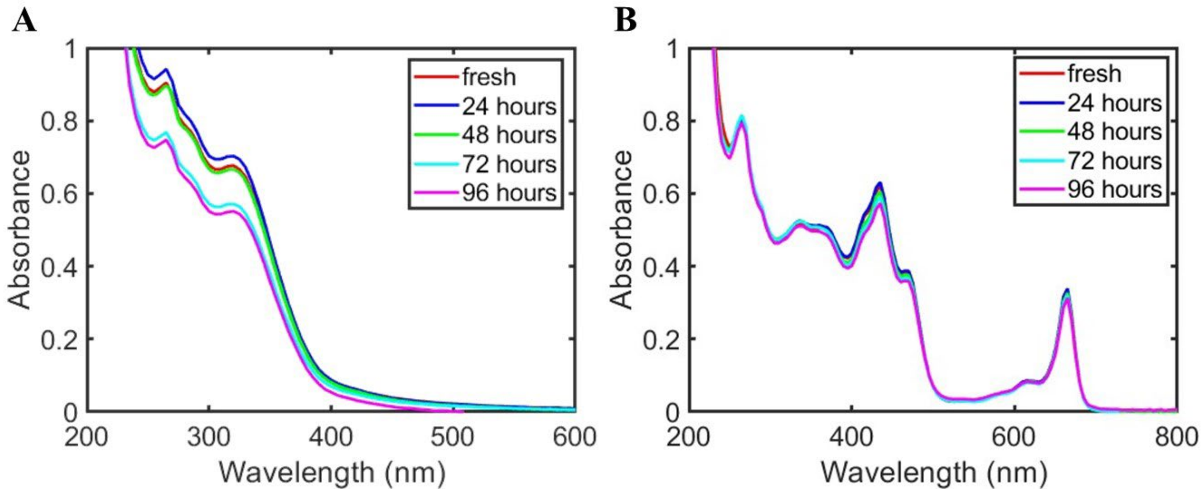

Figure S4. Absorbance spectra of (A) an aqueous kudzu leaf extract and (B) an ethanolic kudzu leaf extract acquired in 24 h increments over five days to monitor the compositional stability of the extract.

Table S1. The pH of an aqueous kudzu leaf extract was monitored in 24 h increments over five days.

Extract Age	pH
0 h	**6.1**
24 h	**6.1**
48 h	**6.1**
72 h	**6.1**
96 h	**6.1**

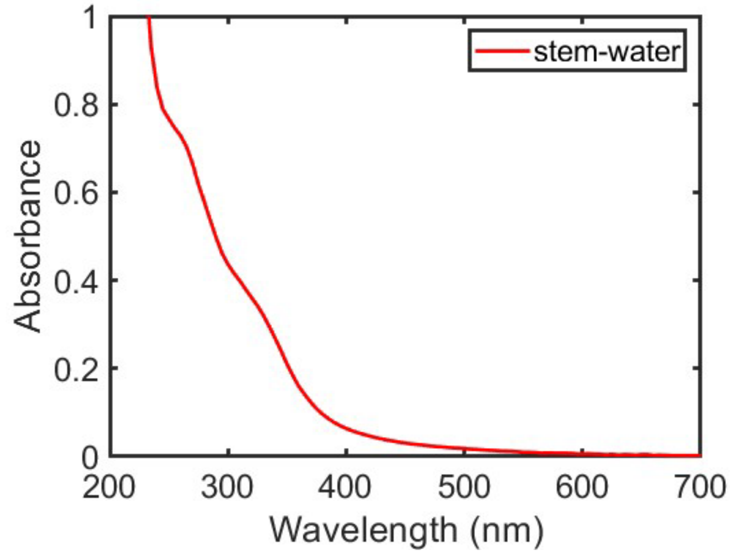

Figure S5. Absorbance spectra of an aqueous kudzu stem extract.

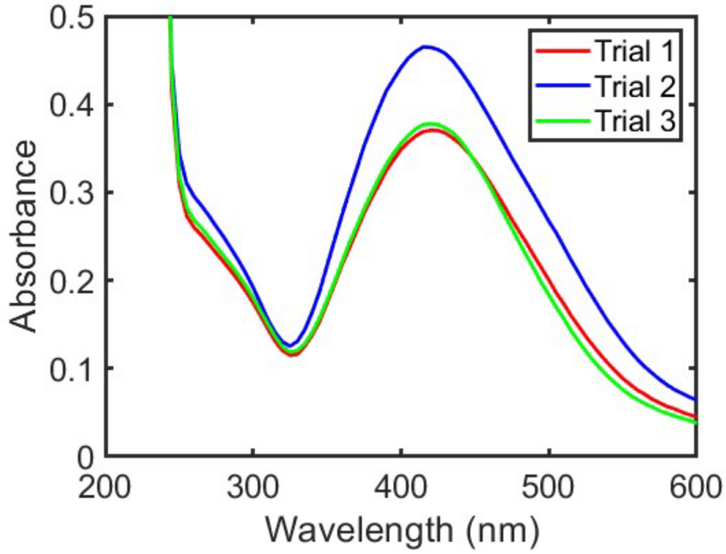

Figure S6. Absorbance spectra of Ag nanoparticles synthesized with an aqueous kudzu stem extract. The stem extract is characterized in Figure S5.

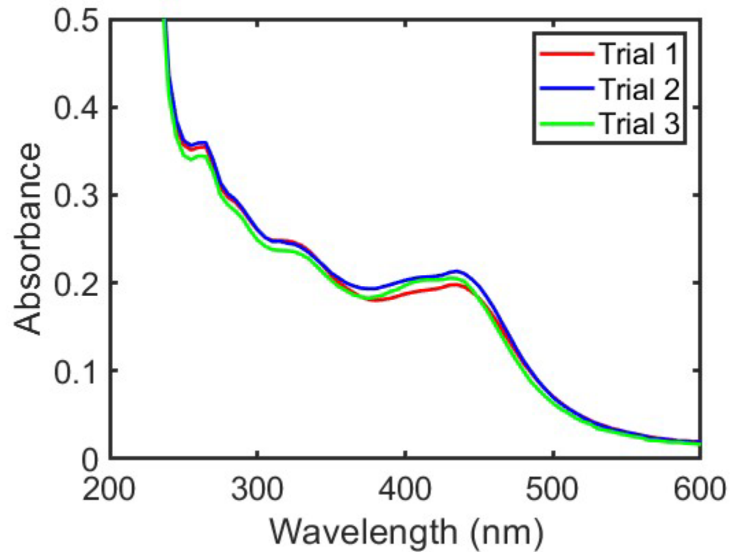

Figure S7. Absorbance spectra of Ag nanoparticles synthesized with kudzu leaf extract prepared using a solvent composed of equal volumes of H_2O and CH_3CH_2OH.

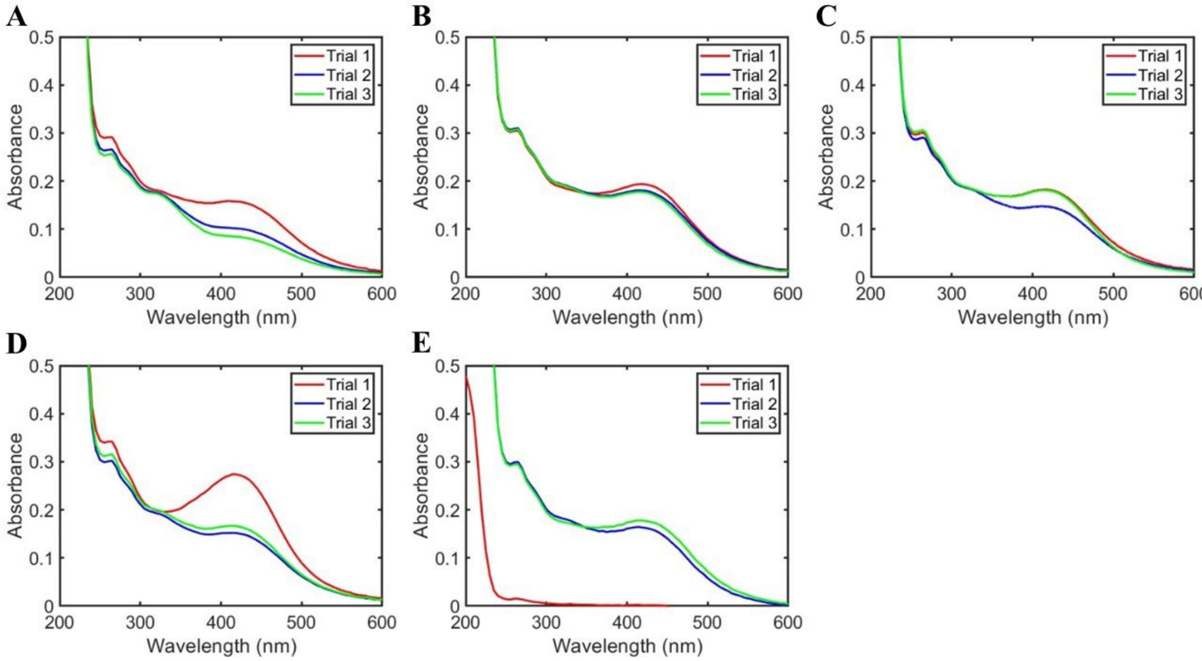

Figure S8. Absorbance spectra of Ag nanoparticle colloids synthesized by adding 3 mL of aqueous kudzu leaf extract and 1.5 mL of 0.04 M $AgNO_3$ to 95.5 mL of H_2O and boiling the solution. The aqueous extract used is characterized in Figure S4A. Ag nanoparticles were synthesized in triplicate using aqueous extract that was aged (A) 0 h, (B) 24 h, (C) 48 h, (D) 72 h, and (E) 96 h.

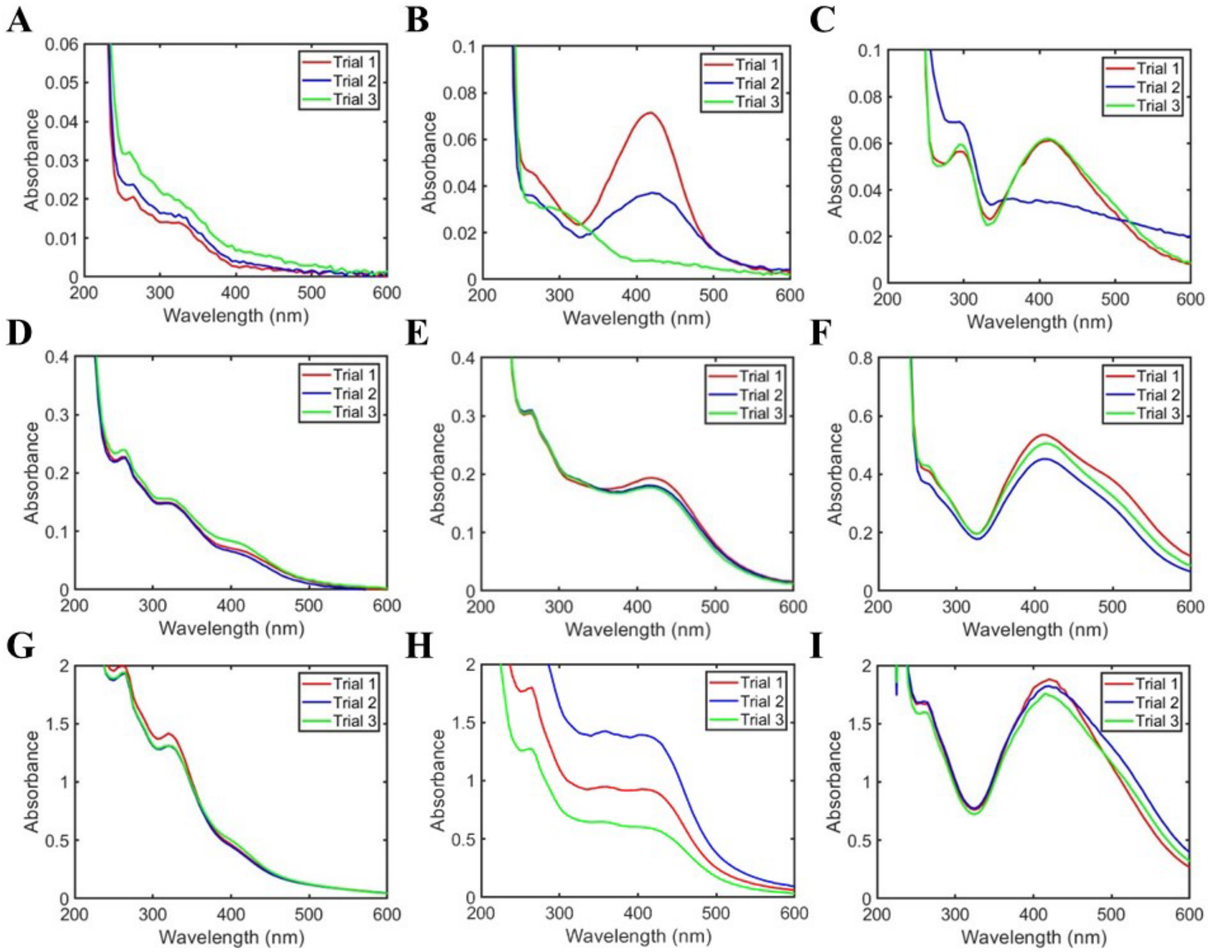

Figure S9. Absorbance spectra of Ag nanoparticle colloids synthesized using different concentrations of $AgNO_3$ and aqueous kudzu leaf extract. Syntheses were carried out in triplicate in an aqueous solution with each of the following final reactant concentrations: (A) 0.2 %v/v aqueous extract and 39.9 μM $AgNO_3$, (B) 0.2 %v/v aqueous extract and 0.40 mM $AgNO_3$, (C) 0.2 %v/v aqueous extract and 3.6 mM $AgNO_3$, (D) 2.0 %v/v aqueous extract and 39.2 μM $AgNO_3$, (E) 1.9 %v/v aqueous extract and 0.39 mM $AgNO_3$, (F) 1.8 %v/v aqueous extract and 3.6 mM $AgNO_3$, (G) 16.7 %v/v aqueous extract and 33.3 μM $AgNO_3$, (H) 16.5 %v/v aqueous extract and 0.33 mM $AgNO_3$, and (I) 15.4 %v/v aqueous extract and 3.1 mM $AgNO_3$.

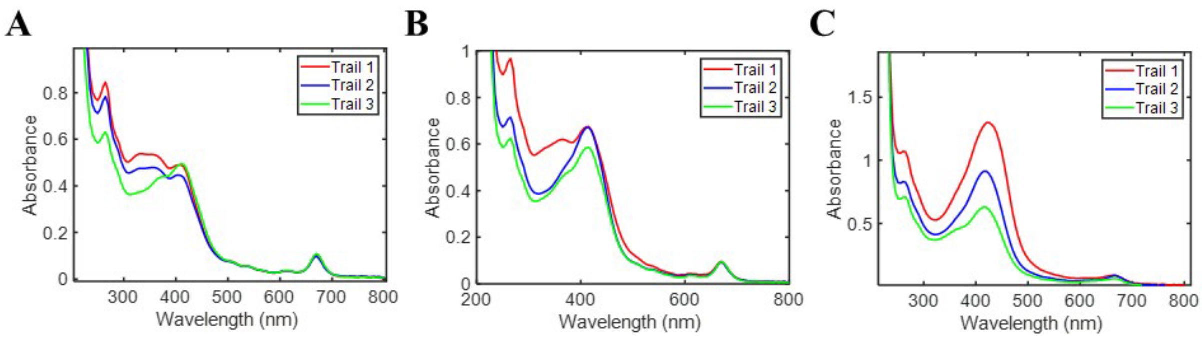

Figure S10. Absorbance spectra of Ag nanoparticle colloids synthesized using ethanolic kudzu leaf extract and different concentrations of $AgNO_3$. Syntheses were carried out in triplicate in an aqueous solution with each of the following final reactant concentrations: (A) 16.5 %v/v ethanolic extract and 33 μM $AgNO_3$, (B) 16.5 %v/v ethanolic extract and 0.33 mM $AgNO_3$, and (C) 16.5 %v/v ethanolic extract and 3.3 mM $AgNO_3$.

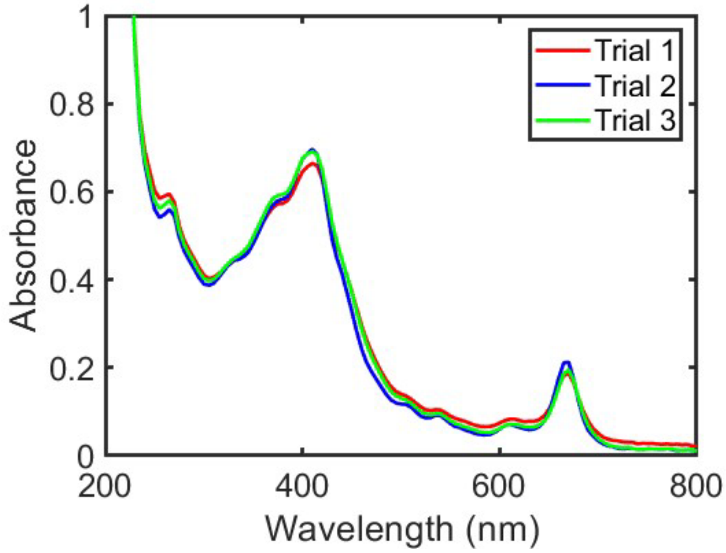

Figure S11. Absorbance spectra of three trials of Ag nanoparticle synthesis using final concentrations of 0.33 mM $AgNO_3$ and 16.5 %v/v mL of ethanolic kudzu leaf extract as the reducing agent.

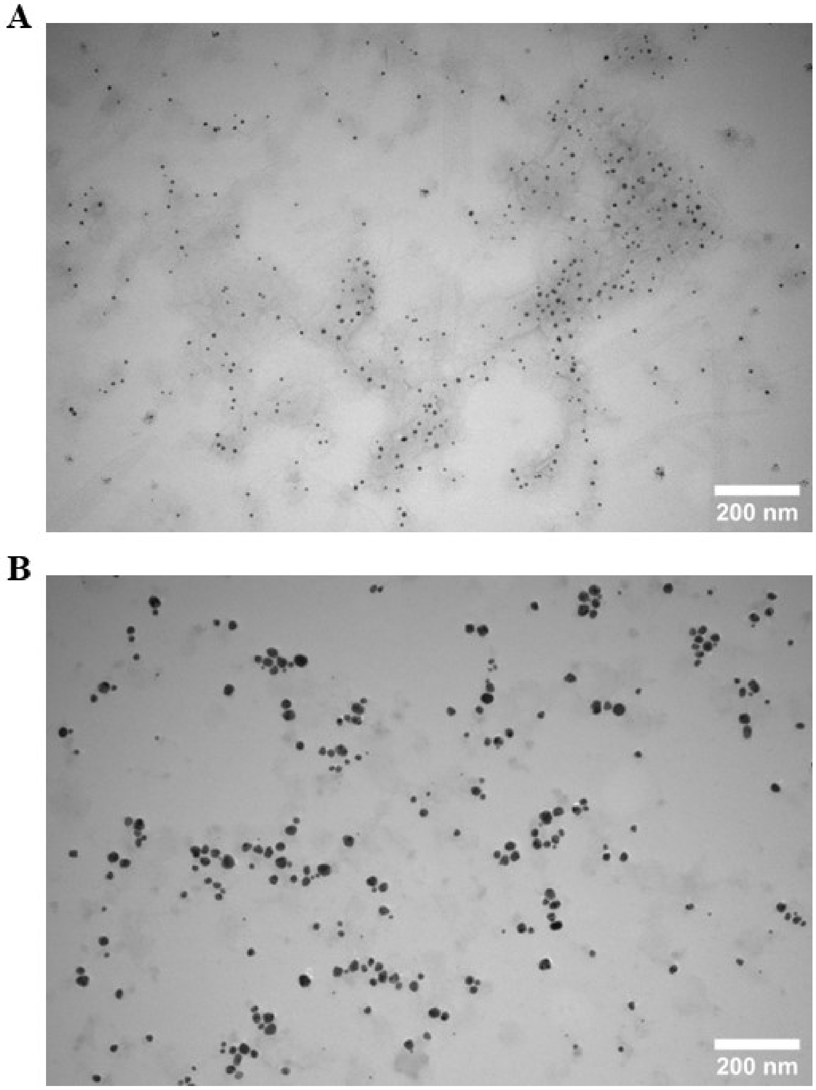

Figure S12. Additional TEM images of Ag nanoparticles synthesized with (A) CH_3CH_2OH-based kudzu leaf extract and (B) H_2O-based kudzu leaf extract.

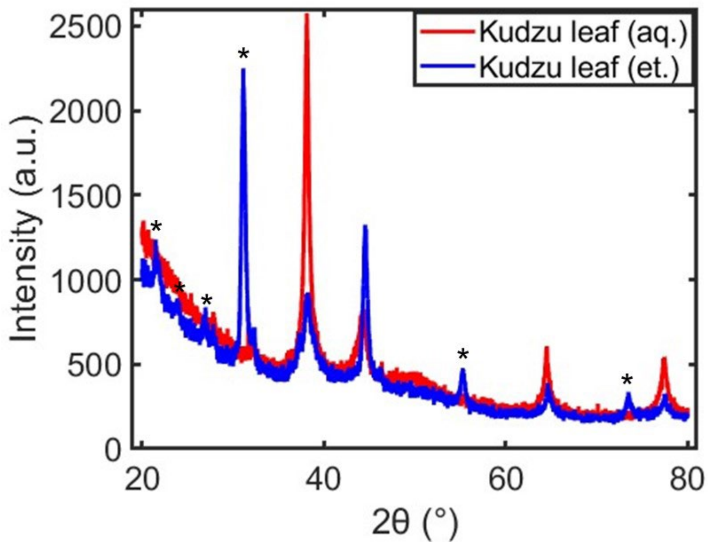

Figure S13. Powder X-ray diffraction data of Ag nanoparticles synthesized with aqueous (red) and ethanolic (blue) kudzu leaf extracts. Nanoparticles from ethanolic extract (blue) show additional peaks, marked by asterisks, which are likely due to unreacted $AgNO_3$.

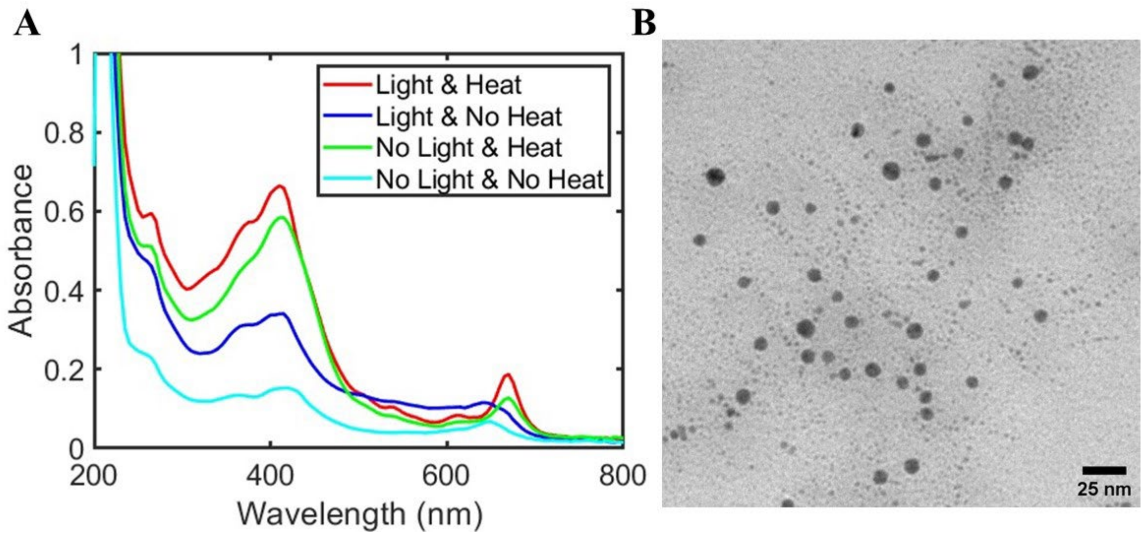

Figure S14. (A) Absorbance spectra of Ag nanoparticles synthesized in ambient light with (red curve) and without (dark blue curve) heat and in dark conditions with (green curve) and without (light blue curve) heat using final concentrations of 0.33 mM $AgNO_3$ and 16.5 %v/v mL of ethanolic kudzu leaf extract as the reducing agent. Without heat, the chlorophyll is exposed to Ag^+ for a prolonged period resulting in degradation of chlorophyll evidenced by the change in the electronic resonance peaked at 665 nm to 650 nm. (B) Representative TEM image of Ag nanoparticles synthesized in dark conditions with heat using 0.33 mM $AgNO_3$ and 16.5 %v/v mL of ethanolic kudzu leaf extract.

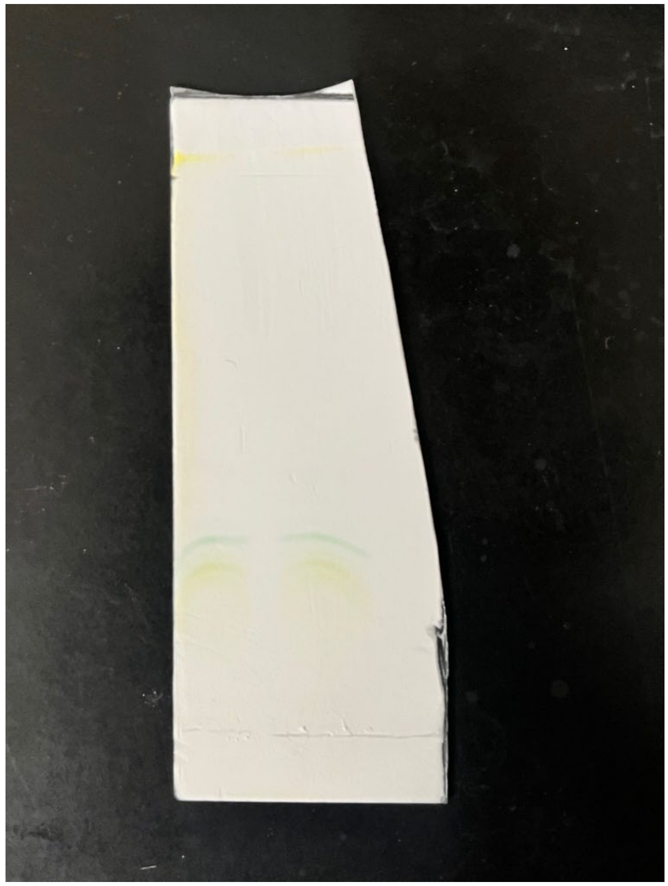

Figure S15. Glass thin-layer chromatography plate showing results from the ethanolic kudzu leaf extract. Retention factors of the separated components are 0.30 and 0.36, respectively.

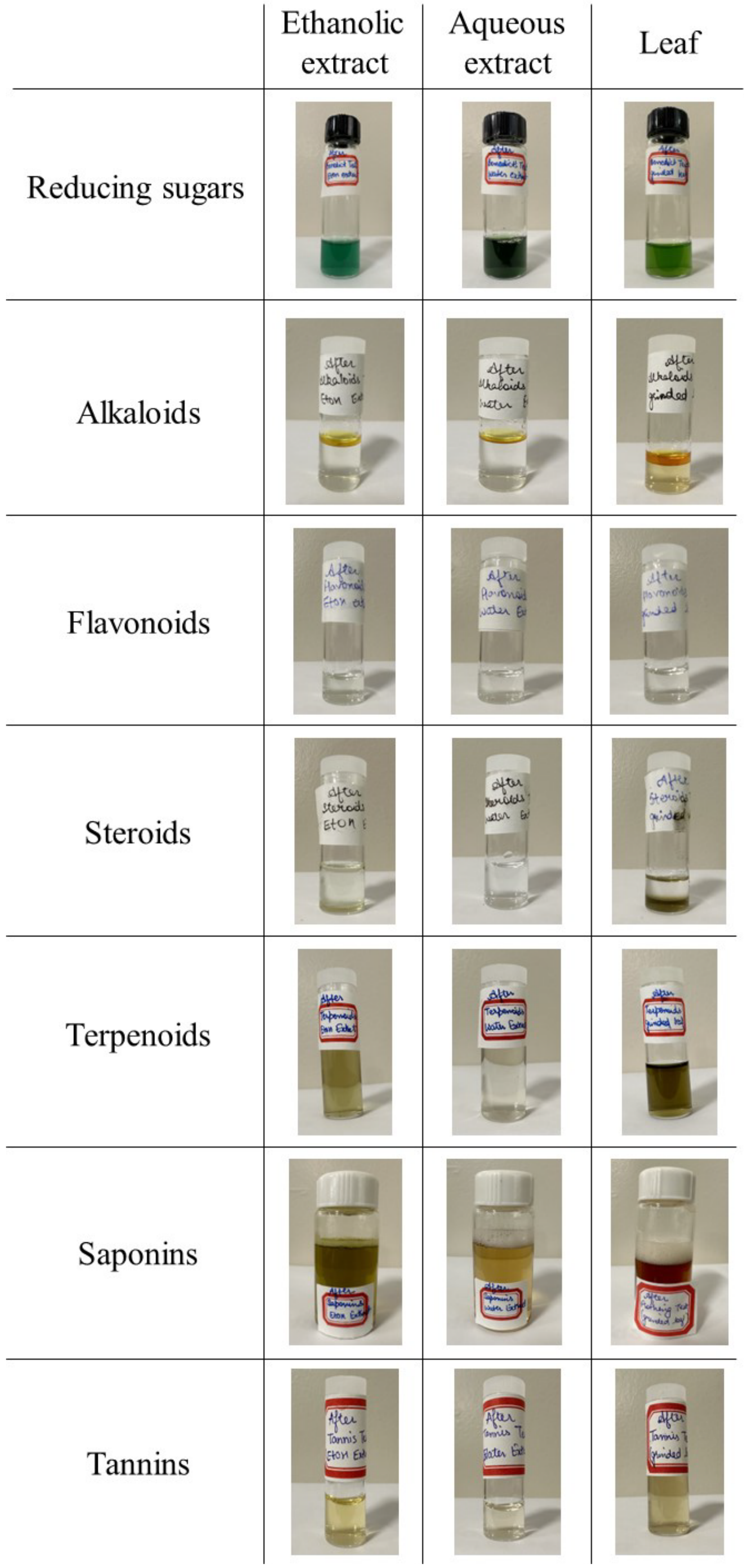

Figure S16. Representative photographs of reaction mixtures after screening for reducing sugars, alkaloids, flavonoids, steroids, terpenoids, saponins, and tannins in ethanolic kudzu leaf extract (left column), aqueous kudzu leaf extract (middle column), and kudzu leaves (right column).

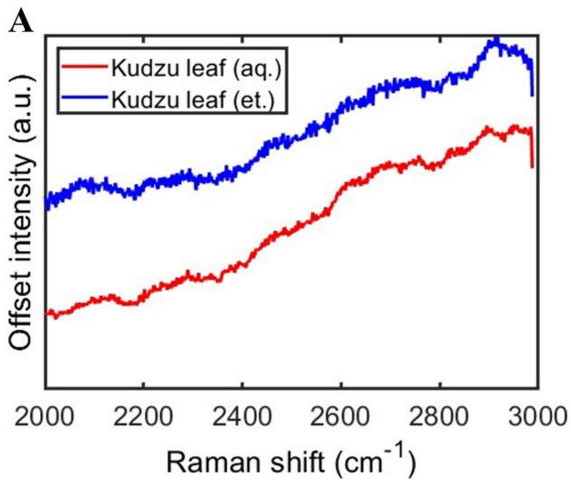

Figure S17. Surface-enhanced Raman scattering in the (A) mid- and (B) high wavenumber regions from aggregated Ag nanoparticles synthesized with ethanolic (blue) and aqueous (red) kudzu leaf extracts.

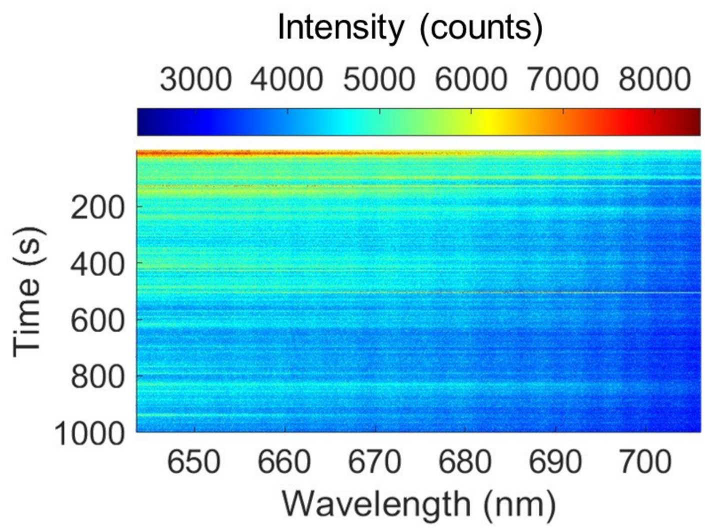

Figure S18. Waterfall plot showing spectra from the surface of Ag nanoparticles synthesized with an aqueous kudzu leaf extract. No chlorophyll fluorescence is observed.